Molecular Nanoswitches

DOI: 10.1002/anie.201202759

The Carboxylate Twist: Hysteretic Bistability of a High-Spin Diiron(II) Complex Identified by Mössbauer Spectroscopy**

*Boris Burger, Serhiy Demeshko, Eckhard Bill, Sebastian Dechert, and Franc Meyer**

Dedicated to Professor Dieter Fenske on the occasion of his 70th birthday

Carboxylates have always been among the most versatile and thus widely used ligands in coordination chemistry.[1] On account of their various possible modes of coordination, both terminal and bridging, they form a wide range of mono- and polynuclear complexes and are often found as ligands in metalloproteins. Facile interconversion between carboxylate binding modes, termed the carboxylate shift, is implicated as a critical step in many enzymatic reactions and is known to play a fundamental role in the catalytic cycles of, for example, soluble methane monooxygenase (sMMO) and the R2 subunit of ribonucleotide reductase (RNR R2).[2] Just recently, we reported a pyrazolate-based[3] diiron(II) complex in which the carboxylate shift could be observed in the solid state for the first time.[4] We reasoned that further exploration of this novel class of diiron(II) carboxylate cores may yield more detailed insight into carboxylate dynamics beyond the common carboxylate shift. Herein we describe a new bioinspired high-spin (μ-pyrazolato)(μ-carboxylato)diiron(II) complex **1** based on the bis(tetradentate) ligand HL (Figure 1).[5] Complex **1** features pronounced conformational flexibility of the exogenous acetato ligand[6] which gives rise to an unprecedented thermal hysteresis, identified by Mössbauer spectroscopy and SQUID magnetometry (SQUID = superconducting quantum interference device). This hysteresis does not involve any spin transition or any configurational change and is hence a borderline case of the well-known carboxylate shift. We will coin the underlying process the "carboxylate twist".

Switchable molecule-based materials are indeed expected to have great potential for future data-storage and sensing applications. Hence there is much interest in molecular systems that show hysteretic bistability near room temperature, with the spin-crossover[7] and valence tautomeric compounds[8] probably being the most prominent examples. In the case of iron complexes, Mössbauer spectroscopy has proven to be a valuable tool for investigating the effects associated with bistability.[7c,9] However, hysteretic behavior distinct from spin crossover has not yet been observed for iron complexes, and hence has not yet been investigated by Mössbauer spectroscopy.

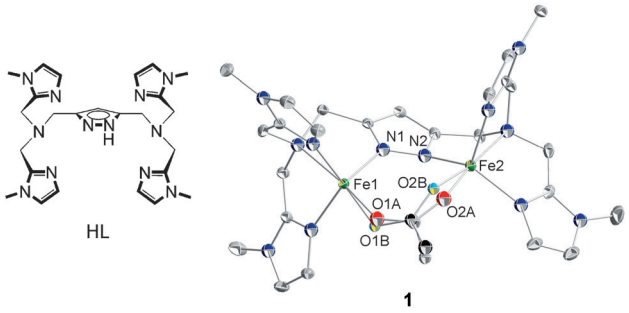

Figure 1. Ligand HL and the molecular structure of the cation of **1** (133 K).

We previously reported a (μ-azido)(μ-pyrazolato)dinickel(II) complex which showed thermal magnetic bistability induced by a twist of the bridging azido coligand along the Ni-NNN-Ni dihedral angle, turning the antiferromagnetic exchange coupling on and off.[10] This behavior gives rise to an unprecedented hysteresis, clearly distinct from spin crossover and valence tautomerism scenarios. It is worth noting that there are only a handful of other examples reported in the literature where a subtle geometric distortion induces bistability and hysteresis without any spin or redox transitions.[11] Novel effects are now observed in the new pyrazolato-bridged diferrous complex **1** in which a flexible carboxylate is clamped between the metal centers.

The reaction of HL with a mixture of $Fe(OAc)_2$ and $Fe(OTf)_2{\cdot}2\,MeCN$ (OTf = trifluoromethanesulfonate) in MeCN gave the *syn-syn* bidentate μ_2-η^1:η^1 acetate-bridged complex $[LFe^{II}_2(\mu\text{-}OAc)](OTf)_2$ (**1**), which is highly air and moisture sensitive (all experimental details are given in the Supporting Information). The molecular structure of the cation of **1** at 133 K, determined by X-ray diffraction, is shown in Figure 1. Complex **1** crystallizes in the triclinic space group $P\bar{1}$ with one cation and two triflate anions within the asymmetric unit. The two crystallographically independent Fe ions in **1** are both found in distorted trigonal-bipyramidal $\{N_4O\}$ environments, comprising the tetradentate binding pocket of the pyrazole ligand and an O atom of the μ-acetate.

[*] B. Burger, Dr. S. Demeshko, Dr. S. Dechert, Prof. Dr. F. Meyer
Institut für Anorganische Chemie
Georg-August-Universität Göttingen
Tammannstrasse 4, 37077 Göttingen (Germany)
E-mail: franc.meyer@chemie.uni-goettingen.de
Homepage: http://www.meyer.chemie.uni-goettingen.de
Dr. E. Bill
Max-Planck-Institut für Bioanorganische Chemie
Stiftstrasse 34–36, 45470 Mülheim an der Ruhr (Germany)

[**] Financial support by the DFG (International Research Training Group 1422 "Metal Sites in Biomolecules: Structures, Regulation and Mechanisms"; see www.biometals.eu) and the Evonik Foundation (PhD fellowship for B.B.) is gratefully acknowledged.

Supporting information for this article is available on the WWW under http://dx.doi.org/10.1002/anie.201202759.

The acetate ligand is disordered over two positions with some variation in the dihedral angles Fe1-O1···O2-Fe2.

Magnetic susceptibilities of single crystals of **1** were measured in the range between 2 and 295 K and showed an unexpected, broad, and asymmetric magnetic hysteresis of about 0.4 $cm^3 K mol^{-1}$ centered at $T_{1/2}\downarrow \approx 140$ and $T_{1/2}\uparrow \approx 230$ K (Figure 2). As will be shown later, this is associated

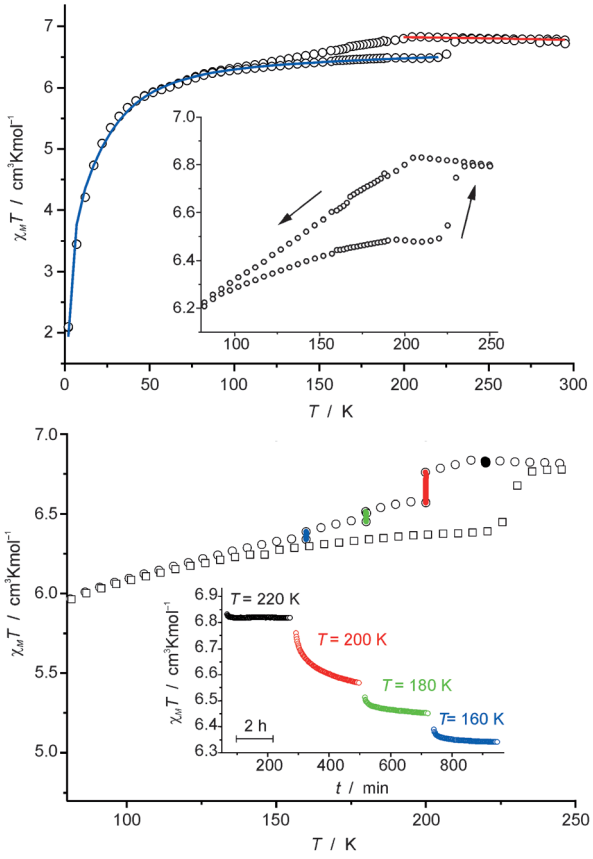

Figure 2. Top: Temperature dependence of $\chi_m T$ for **1** illustrating the thermal magnetic hysteresis between 205 and 225 K (expanded in inset). The blue and red curves correspond to a simulation with weak antiferromagnetic coupling and varying contribution of the orbital angular momentum ($g = 2.171$ (red) and $g = 2.073$ (blue)). Bottom: Time (inset) and temperature dependence of $\chi_m T$ in the hysteresis region in measurements with isothermal intervals.

with a twist of the bridging acetate ligand which distorts the environment of the two iron atoms. Mössbauer experiments (see below) provide evidence that the ferrous ions remain in their high spin state throughout. Thus the magnetization change is not caused by a change of spin contribution to the magnetic susceptibility and therefore cannot be explained by a conventional spin-crossover mechanism.

At temperatures above 205 K the $\chi_m T$ value of **1** is 6.8 $cm^3 K mol^{-1}$, which is somewhat higher than the spin-only value for two uncoupled high-spin iron(II) ions (6.0 $cm^3 K mol^{-1}$ for $g = 2.00$). This indicates that a minor contribution of the angular momentum is present within that temperature range, reflected in a g value of 2.073, that is, slightly larger than 2.0023. At approximately 205 K the $\chi_m T$ curve in the first cooling scan of a single crystal of **1** shows an abrupt change in slope (Figure 2). The decrease in $\chi_m T$ in the slow cooling scan is associated with a structural phase transistion that results in partial loss of crystallinity and disintegration of the single crystal, most likely induced by a twist of the bridging acetate ligand at the molecular level. At around 80 K the $\chi_m T$ curve reaches a value of 6.2 $cm^3 K mol^{-1}$. Below this point the temperature dependence can be readily described by the combined effect of single-ion zero-field splitting and antiferromagnetic exchange coupling. When the temperature is subsequently increased, the $\chi_m T$ curve shows a progression different from the cooling scan and opens a broad hysteresis at around 80 K. $\chi_m T$ reaches values that are about 0.3 to 0.4 $cm^3 K mol^{-1}$ below the values measured in the cooling scan, until an abrupt and steep increase of $\chi_m T$ at around 230 K closes a full hysteretic cycle. The curves are almost superimposed above 235 K, reaching 6.8 $cm^3 K mol^{-1}$ at 295 K. Time-dependent isothermal susceptibility measurements revealed that the drop in $\chi_m T$ below 205 K is a very slow process; thus the $\chi_m T$ value decreases over the course of hours at constant temperature. This results in a steplike curve in the time domain (Figure 2 and Figure S3 in the Supporting Information). In the second cycle the shape and course of the hysteresis curve changes significantly, in combination with a thermal memory effect. This phenomenon is not yet fully understood and currently being investigated.

For comparison a second system, a solvate of **1** (namely **1**·2 MeCN, $[LFe_2(\mu\text{-}OAc)](OTf)_2 \cdot 2\,MeCN$), has been investigated by means of magnetic susceptibility measurements. The molecular structure of **1**·2 MeCN (see Figure S6 in the Supporting Information) did not show any disorder of the acetate moiety in the solid state. Moreover the dihedral angle around the acetate moiety did not show a significant alteration with temperature. Magnetic susceptibility measurements on **1**·2 MeCN accordingly did not indicate any unusual or unexpected behavior and could be well simulated with the parameters given in Table S1 in the Supporting Information. Hysteretic behavior is clearly not observed for this system, which is very similar to **1** but includes solvent molecules in the crystal lattice.

In accordance with the transition temperatures determined from SQUID data, differential scanning calorimetric (DSC) measurements on large single crystals of **1** display a diffuse exothermic signal between 210 and 190 K in the cooling mode, and a sharp endothermic signal at 230 K in the warming mode (see Figure S5 in the Supporting Information). The diffuse nature of the former is likely due to disintegration of the large crystals upon slow cooling below the destructive phase transition.

Because of the loss of crystallinity, it was not possible to determine the molecular structure of slowly cooled crystals of **1** at temperatures below 213 K. However, flash freezing of small single crystals in the cryostream of the diffractometer is nondestructive and diffraction data for **1** was collected at temperatures below the phase transition. In magnetic susceptibility measurements on a flash-frozen crystalline sample the $\chi_m T$ curve in the warming mode is identical to that in Figure 2 which was measured for a slowly cooled sample. This confirms that the structures determined in the warming mode

using a flash-frozen crystal indeed represent the original warming cycle of the $\chi_m T$ progression. The crystal structure of **1** has thus been determined in several steps in the temperature range progressing from 82 K to 258 K for several crystals (see the Supporting Information). Major variations are mainly observed for the disordered bridging acetate ligand, though individual occupancy factors for the two refined positions are close to 50:50 throughout the full temperature range (see the Supporting Information). In addition to the observed disorder, the bridging acetate undergoes substantial temperature-dependent movement in the solid state. The dihedral angles Fe1-O1···O2-Fe2 for both refined positions show a remarkable quasilinear increase with increasing temperature, displaying an alteration of up to 70° from 82 to 258 K. (Figure 3). An overlay of the molecular

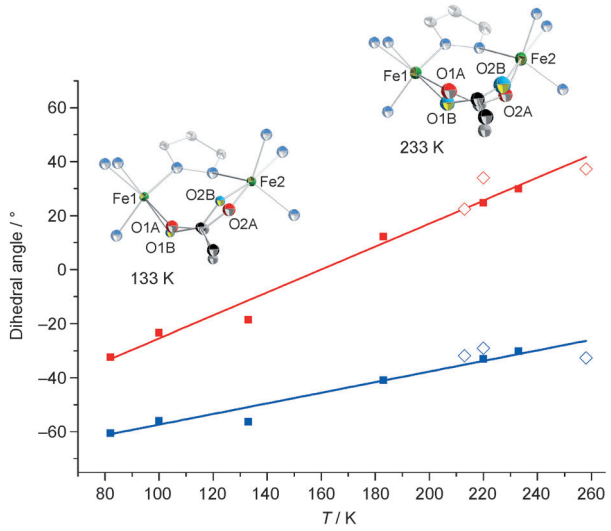

Figure 3. Temperature dependence of the dihedral angles Fe–O···O–Fe of the acetate conformers A and B and illustration of the diiron carboxylate core structures at 133 K and 233 K. Red squares: conformer A measured in heating mode; red diamonds: conformer A measured in cooling mode; blue squares: conformer B measured in heating mode; blue diamonds: conformer B measured in cooling mode. Red and blue solid lines represent linear regression fits.

structures at 133 and 233 K (obtained from diffraction data of the same crystal) can be found in the Supporting Information (Figure S10) for one of the disorder conformers. The topology of the coordinating ligand scaffold as well as the relative positions of the iron centers remain almost constant whilst the acetate ligand makes a significant twist at higher temperature. It is noteworthy that the dihedral angle Fe1-N1-N2-Fe2 involving the pyrazolate is much less sensitive to temperature changes and shows an alteration of only around 6° between 133 and 233 K.

Raman spectra of a solid crystalline sample of **1** at different temperatures in the range of interest are depicted in Figure 4. The signals observed in the region of the asymmetric COO^- stretching and CH_3 deformation vibrations between 1300 and 1500 cm^{-1} are clearly different at 258/203 K and 133 K, corroborating conformational changes of the μ-acetate. Though crystallinity is lost after the first measurement in

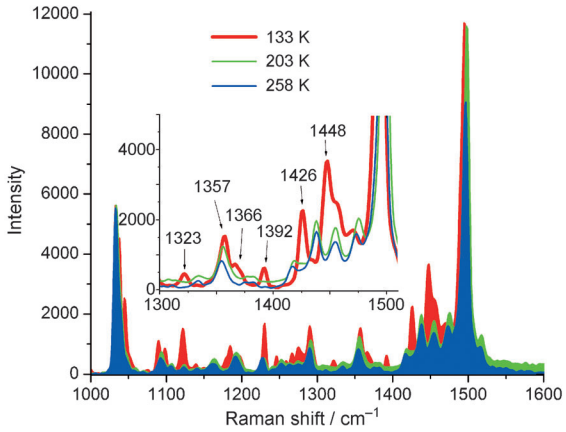

Figure 4. Raman spectra of single crystals of **1** at different temperatures. The inset highlights the relevant changes in the spectra.

the cooling mode, the changes are fully reversible on the Raman timescale.

At this point, the available data did not provide a clear explanation of the hysteretic behavior but remained somewhat conflicting, as the magnetic measurements show abrupt changes whilst the diffraction data suggest a quasilinear continuous variation. These findings prompted us to study this system in more detail using Mössbauer spectroscopy. Some intriguing Mössbauer spectra for a crystalline sample of **1** in the temperature range from 80 to 260 K are depicted in Figure 5. All corresponding Mössbauer parameters are listed in Table 1.

Only one sharp, widely split quadrupole doublet is observed at 80 K (Figure 5, spectrum 1). With increasing temperature the absorption lines slightly broaden (spec-

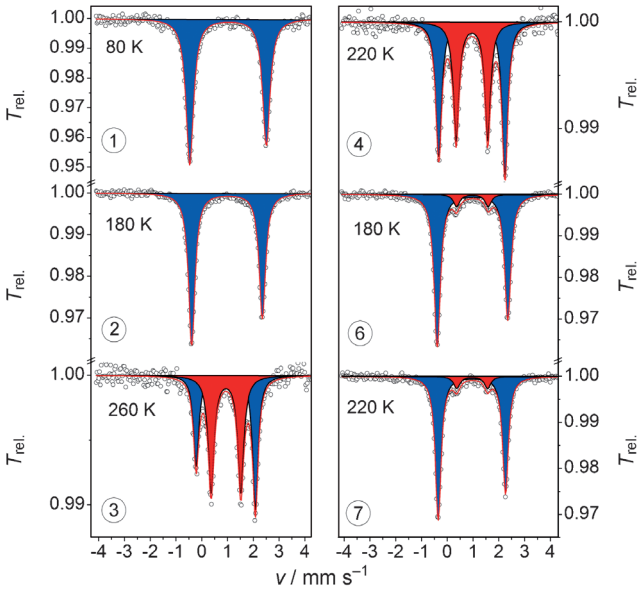

Figure 5. Selected Mössbauer spectra of **1** at various temperatures. The lines represent simulations with Lorentzian doublets of equal line widths for high- and low-energy lines, but with different intensities, taking heterogeneity into account. Numbers correspond to the measurement sequence shown in Figure 6.

Table 1: Mössbauer parameters for the spectra shown in Figure 5. (a: static (blue doublet), b: dynamic (red doublet); cases a and b both involve the two conformers A and B.)

T [K]	δ_{exp}, a/b	$\lvert\Delta E_Q\rvert$ a/b	Γ_{FWHM}, a/b	$I_{rel.}$
80	1.02	2.97	0.35	100
180	0.98	2.74	0.30	100
260	0.93/0.94	2.30/1.15	0.25/0.28	46.2/53.8
220	0.96/0.96	2.57/1.22	0.27/0.28	54.5/45.5
180	0.98/0.98	2.74/1.23	0.30/0.30	91.7/8.3
220	0.96/0.97	2.61/1.19	0.27/0.30	90.6/9.4

[a] δ = isomer shift, Γ_{FWHM} = full width at half maximum, $I_{rel.}$ = relative intensity.

trum 2), until the spectrum splits into two separate sharp quadrupole doublets that reach relative intensities of 46.2% ($|\Delta E_Q|$=2.30 mm s^{-1}) and 53.8% ($|\Delta E_Q|$=1.15 mm s^{-1}) at 260 K (spectrum 3). A subsequent measurement in the cooling mode reveals hysteretic behavior with respect to the intensity of the inner quadrupole doublet (Figure 6). A drastic

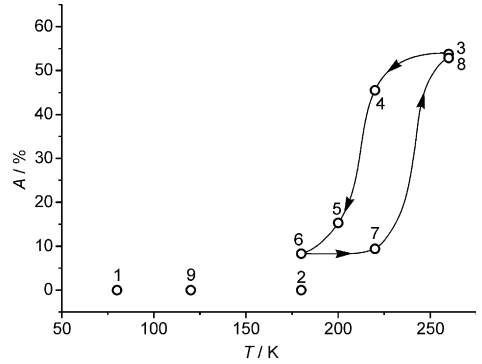

Figure 6. Thermal hysteresis of the intensity of the inner doublet in the Mössbauer spectra of a crystalline sample of **1** during the first cycle (80 K→260 K→180 K→260 K). Numbers correspond to spectra in Figure 5.

decrease of intensity is observed between 220 and 180 K until only around 8% of the intensity remains for the inner doublet (4→6). Subsequent warming to 220 K (6→7) does not cause any change in the relative intensities, clearly indicating hysteretic behavior. Further warming to 260 K then leads to a sudden increase in intensity for the inner doublet with final proportions at 260 K of around 47.1% ($|\Delta E_Q|$=2.29 mm s^{-1}) and 52.9% ($|\Delta E_Q|$=1.14 mm s^{-1}). This completes a full hysteresis loop (a full set of spectra can be found in the Supporting Information).

The reason for the appearance of a second Mössbauer quadrupole doublet with a remarkably small quadrupole splitting at higher temperatures is not immediately clear, as the metric parameters of the two independent iron ions in **1** seem to become more similar with increasing temperature. Counterintuitively, the two iron atoms exhibit slightly differing coordination geometries at low temperature, where only one quadrupole doublet is present, whereas they become more alike at higher temperatures where two distinct Mössbauer spectra are observed. Apparently the dihedral angle Fe1–O1···O2–Fe2 obtained in a static description of the molecular structures of **1** cannot explain the dramatic difference in the quadrupole splittings of about 2 mm s^{-1} for the iron sites. Thus we have to take dynamic effects into account. We suggest that two conformers of **1** as identified by refinement of the diffraction data give rise to an equilibrium between two distinct species (with different Fe–O···O–Fe torsion angles) in the solid state, over the whole temperature range under investigation. Although the metric parameters of Fe1 and Fe2 are different at low temperatures, the corresponding electric field gradient (EFG) tensors for the two iron nuclei can differ only in orientation or eventually the sign, but not by the absolute value of their main component, $|V_{zz}|$, since they cause essentially the same quadrupole splitting in the zero-field Mössbauer spectra recorded in the low-temperature region. Specifically, the dihedral angles around the two acetate conformers have the same direction and sign at lower temperatures, but at temperatures above 180 K they are oriented antipodal to the iron–iron vector (see Figure 3 and Figure 7 and Table S6f). We anticipate appreci-

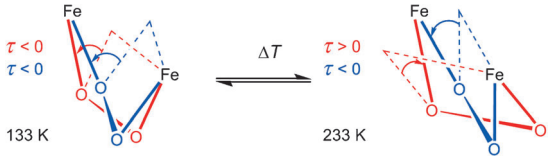

Figure 7. Schematic explanation of the algebraic sign and meaning of the torsion angles τ (red: conformer A, blue: conformer B, according to Figure 3).

able misalignment of the EFGs for each of the iron sites in these two conformations, since the strong valence contribution to the EFG arising from the 3d^6 configuration may amplify the effect of even relatively subtle topological changes for the resulting EFG. In this situation, the onset of fast dynamic interconversion of the two conformations can induce pronounced temperature dependence of the observed quadrupole splitting for each iron site. If the realaxtion rate is fast compared to the nuclear lifetime and quadrupole precession rate, the component-wise averaged EFG tensor is experienced by the Mössbauer nuclei,[12] such that in the extreme case of opposite signs for the tensor components the quadrupole splitting can even completely collapse.[13]

Along these lines, we suggest that complex **1** shows "static disorder" at lower temperatures, such that the two conformations yield identical subspectra with the same large quadrupole splitting for both iron sites. At temperatures above 180 K dynamic interconversion of the two conformers sets in, causing fast fluctuations of the EFG for both iron sites. As a consequence, the average of the static tensors gives rise to a new quadrupole doublet with much smaller splitting, which abruptly gains intensity above 220 K, in good agreement with the sharp increase of the $\chi_m T$ curve observed in the warming mode at roughly 225 K. The corresponding structural transformation from static to dynamic disorder cannot be distinguished by X-ray crystallography since time and ensemble averages are indistinguishable. The diffraction experiments

provide information about vibration amplitudes of the acetate, whereas the Mössbauer experiments reveal the dynamic interconversion of the local iron environments within a typical time window of 10^{-7} s. The X-ray data did not indicate any change in unit cell symmetry as a function of temperature, nor did we find any possibility to explain the data by adopting a larger unit cell, as the cell choice was unique and not affected by temperature. Although hysteretic behavior depends essentially on cooperative phenomena in the solids, it is not trivial to identify corresponding pathways for intermolecular interactions. A survey of direct contacts between cations as well as cations and anions in the crystal structure of **1** at different temperatures is found in the Supporting Information.

The ratio of statically and dynamically disordered bulk material may depend on several factors including the particular solid-state domains, size and shape of the crystallites, internal pressure and, of crucial importance, temperature. Thus, it is not surprising that the Mössbauer subspectrum, reflecting the dynamically disordered part, gains intensity with increasing temperature and even constitutes the major component above 260 K.

In order to support these findings we performed DFT calculations for the two disorder conformers of **1** that were identified in the solid-state structure (see the Supporting Information for details on the calculations). The EFG tensors calculated for the individual iron nuclei of the two disorder conformers of **1** at 233 K in fact differ primarily in the orientation of their principal axes and the sign of the main components. Although the values cannot fully explain the experimenal differences in the static and dynamic Mössbauer spectra, the resulting averages of the calculated tensor elements indeed yield a significantly lower EFG with smaller $|\Delta E_Q|$ values. The results corroborate our proposal of a fluctuating EFG, in so far as they reveal a distinct dependence of the EFG on the orientation of the coordinating acetate moiety. It is worth noting that averaging the individual EFG tensors for the two disorder conformers at low temperature does not give a reduced $|\Delta E_Q|$ (see the Supporting Information for additional information), since the torsion angles have the same algebraic sign and are almost alike in the low-temperature limit (Table S6).

In conclusion we have discovered a unique pyrazolate-based diiron(II) complex that shows an unprecedented form of hysteretic bistability manifested in magnetic susceptibility data and Mössbauer spectra as well as in structural variations. The effect is not associated with any spin transition, but results from the temperature-dependent dynamic reorientation of a metal-bridging carboxylate ligand, here called the "carboxylate twist". The "carboxylate twist" is distinct from the well-established "carboxylate shift", as it does not involve a change of the carboxylate coordination mode, but a toggle movement of the μ-acetate in the clamp of two metal ions. It is conceivable that such dynamics may contribute to the unique reactivity patterns at carboxylate-bridged dinuclear metalloenzyme active sites. Interestingly, this appears to be the first report of dynamic hysteretic behavior, distinct from spin crossover, which has been observed and identified by Mössbauer spectroscopy.

Received: April 10, 2012
Revised: June 15, 2012
Published online: September 10, 2012

Keywords: carboxylate ligands · dinuclear complexes · iron complexes · magnetic properties · Mössbauer spectroscopy

[1] a) C. J. Carrell, H. L. Carrell, J. Erlebacher, J. P. Glusker, *J. Am. Chem. Soc.* **1988**, *110*, 8651; b) R. C. Mehrotra, R. Bohra, *Metal Carboxylates*, Academic Press, New York, **1983**.

[2] a) R. L. Rardin, W. B. Tolman, S. J. Lippard, *New J. Chem.* **1991**, *15*, 417; b) A. C. Rosenzweig, P. Nordlund, P. M. Takahara, C. A. Frederick, S. J. Lippard, *Chem. Biol.* **1995**, *2*, 409; c) M. Assarsson, M. E. Andersson, M. Högbom, B. O. Persson, M. Sahlin, A.-L. Barra, B.-M. Sjöberg, P. Nordlund, A. Gräslund, *J. Biol. Chem.* **2001**, *276*, 26852; d) B. F. Gherman, M.-H. Baik, S. J. Lippard, R. A. Friesner, *J. Am. Chem. Soc.* **2004**, *126*, 2978; e) M. Högbom, M. E. Andersson, P. Nordlund, *J. Biol. Inorg. Chem.* **2001**, *6*, 315; f) M. Torrent, D. G. Musaev, K. Morokuma, *J. Phys. Chem. B* **2001**, *105*, 322; g) M. E. Andersson, M. Högbom, A. Rinaldo-Matthis, K. K. Andersson, B.-M. Sjöberg, P. Nordlund, *J. Am. Chem. Soc.* **1999**, *121*, 2346.

[3] J. Klingele, S. Dechert, F. Meyer, *Coord. Chem. Rev.* **2009**, *253*, 2698.

[4] B. Burger, S. Dechert, C. Grosse, S. Demeshko, F. Meyer, *Chem. Commun.* **2011**, *47*, 10428.

[5] A. Prokofieva, A. I. Prikhod'ko, E. A. Enyedy, E. Farkas, W. Maringgele, S. Demeshko, S. Dechert, F. Meyer, *Inorg. Chem.* **2007**, *46*, 4298.

[6] M. Alvariño Gil, W. Maringgele, S. Dechert, F. Meyer, *Z. Anorg. Allg. Chem.* **2007**, *633*, 2178.

[7] a) *Topics in Current Chemistry (Spin Crossover in Transition Metal Complexes I–III)* (Eds.: P. Gütlich, H. A. Goodwin), Springer, Berlin, **2004**; b) A. Bousseksou, G. Molnar, L. Salmon, W. Nicolazzi, *Chem. Soc. Rev.* **2011**, *40*, 3313; c) P. Gütlich, A. Hauser, H. Spiering, *Angew. Chem.* **1994**, *106*, 2109; *Angew. Chem. Int. Ed. Engl.* **1994**, *33*, 2024; d) P. Gütlich, Y. Garcia, H. A. Goodwin, *Chem. Soc. Rev.* **2000**, *29*, 419.

[8] a) E. Evangelio, D. Ruiz-Molina, *Eur. J. Inorg. Chem.* **2005**, 2957; b) O. Sato, A. Cui, R. Matsuda, J. Tao, S. Hayami, *Acc. Chem. Res.* **2007**, *40*, 361.

[9] C. M. Grunert, S. Reiman, H. Spiering, J. A. Kitchen, S. Brooker, P. Gütlich, *Angew. Chem.* **2008**, *120*, 3039; *Angew. Chem. Int. Ed.* **2008**, *47*, 2997.

[10] G. Leibeling, S. Demeshko, S. Dechert, F. Meyer, *Angew. Chem.* **2005**, *117*, 7273; *Angew. Chem. Int. Ed.* **2005**, *44*, 7111.

[11] a) S. Zang, X. Ren, Y. Su, Y. Song, W. Tong, Z. Ni, H. Zhao, S. Gao, Q. Meng, *Inorg. Chem.* **2009**, *48*, 9623; b) O. Jeannin, R. Clérac, M. Fourmigué, *J. Am. Chem. Soc.* **2006**, *128*, 14649; c) G. Juhász, R. Matsuda, S. Kanegawa, K. Inoue, O. Sato, K. Yoshizawa, *J. Am. Chem. Soc.* **2009**, *131*, 4560.

[12] C. Herta, H. Winkler, R. Benda, M. Haas, A. X. Trautwein, *Eur. Biophys. J.* **2002**, *31*, 478.

[13] a) G. Carver, C. Dobe, T. B. Jensen, P. L. W. Tregenna-Piggott, S. Janssen, E. Bill, G. J. McIntyre, A. L. Barra, *Inorg. Chem.* **2006**, *45*, 4695; b) S. Mukherjee, T. Weyhermüller, E. Bill, K. Wieghardt, P. Chaudhuri, *Inorg. Chem.* **2005**, *44*, 7099.

